# Supporting Information

## Nature of Molecular Interactions of Peptides with Gold, Palladium, and Pd-Au Bimetal Surfaces in Aqueous Solution

Hendrik Heinz,[1]* Barry L. Farmer,[2] Ras B. Pandey,[3] Joseph M. Slocik,[2] Soumya S. Patnaik,[2] Ruth Pachter,[2] and Rajesh R. Naik[2]

*[1]Department of Polymer Engineering, University of Akron, Akron, Ohio 44325*

*[2]Air Force Research Laboratory, Materials and Manufacturing Directorate, AFRL/RX, Wright-Patterson AFB, Ohio 45433*

*[3]Department of Physics and Astronomy, University of Southern Mississippi, Hattiesburg, MS 39406*

* Corresponding author: hendrik.heinz@uakron.edu

# Report Documentation Page

*Form Approved*
*OMB No. 0704-0188*



| 1. REPORT DATE | 2. REPORT TYPE | 3. DATES COVERED |
|---|---|---|
| **2009** | | **00-00-2009 to 00-00-2009** |

| 4. TITLE AND SUBTITLE | 5a. CONTRACT NUMBER |
|---|---|
| **Nature of Molecular Interactions of Peptides with Gold, Palladium, and Pd-Au Bimetal Surfaces in Aqueous Solution** | 5b. GRANT NUMBER |
| | 5c. PROGRAM ELEMENT NUMBER |
| 6. AUTHOR(S) | 5d. PROJECT NUMBER |
| | 5e. TASK NUMBER |
| | 5f. WORK UNIT NUMBER |
| 7. PERFORMING ORGANIZATION NAME(S) AND ADDRESS(ES) **Department of Polymer Engineering,University of Akron,Akron,OH,44325** | 8. PERFORMING ORGANIZATION REPORT NUMBER |
| 9. SPONSORING/MONITORING AGENCY NAME(S) AND ADDRESS(ES) | 10. SPONSOR/MONITOR'S ACRONYM(S) |
| | 11. SPONSOR/MONITOR'S REPORT NUMBER(S) |

12. DISTRIBUTION/AVAILABILITY STATEMENT
**Approved for public release; distribution unlimited**

13. SUPPLEMENTARY NOTES

14. ABSTRACT

15. SUBJECT TERMS

| 16. SECURITY CLASSIFICATION OF: | | | 17. LIMITATION OF ABSTRACT | 18. NUMBER OF PAGES | 19a. NAME OF RESPONSIBLE PERSON |
|---|---|---|---|---|---|
| a. REPORT **unclassified** | b. ABSTRACT **unclassified** | c. THIS PAGE **unclassified** | **Same as Report (SAR)** | **16** | |

## S1. Further Background on Simulation Methods

In summary, we employ a classical atomistic molecular dynamics approach to analyze specific peptide binding to metal surfaces in comparison with thermochemical, IR, NMR, and TEM measurements (Figure 1). The availability of suitable parameters for biomolecules and recent improvements in the accuracy of parameters for inorganic components by more than one order of magnitude[29,37−41] are thereby very helpful.[32–36] Moreover, modeling at all levels, molecular, coarse-grain, and bioinformatics, is ultimately important in identifying the most suitable peptide sequences for controlled binding and detachment (Figure 1) as the huge number of possible sequences exceeds the number of available sequences in commercial phage libraries by more than a million. Quantum-mechanical approaches indicate approximate trends of the interaction of peptide fragments and a few solvent molecules with parts of a surface, and have shown that covalent interactions with metal surfaces are modest to small.[21,22,24,26,28,31] However, such approaches cannot fully explain the mechanisms of binding due to limitations to static calculations including a few hundred atoms, and neglect of thousands of needed solvent molecules, ions, and dynamics at significant time scales. Some ab-initio results also disagree with each other due to known difficulties with the treatment of van-der-Waals interactions (only in wave-function based techniques) and accurate electrostatics.[29,38,40] A limitation of ab-initio and classical atomistic methods is also the difficulty to include polarization effects on metal surfaces;[42−46] though estimates suggest modest contributions on even surfaces. Coarse-grain approaches can be computationally ~$10^3$ times more efficient and include certain specific peptide-surface interactions.[30] A critical role can also be attributed to bioinformatics approaches such as simple numerical screening functions on the basis of molecular-level insight to help eliminate sequences of undesirable binding strength. The success of such higher-level

approaches, however, yet depends on understanding the nature of the molecular interactions (Figure 1).

## S2. Efficient Computation of Adsorption Energies

The quantitative computation of adsorption energies requires the inclusion of explicit water molecules and ionic solutes due to the formation of spatially oriented hydrogen bonds which change their orientation when peptides (or other adsorbates) move from the solution to the surface. The calculation of adsorption energies also requires an accurate summation of Coulomb interactions on the order of ≤0.1 kcal/mol uncertainty for the entire system (see section S3.3). Under these conditions, we have developed and tested two methods to compute the changes in energy, entropy, and free energy upon adsorption (Figure S1).

**S2.1. Method 1 − Simple Approach.** A conceptually simple approach involves the simulation of the adsorbate on the surface (simulation 1) and in solution (simulation 2) using the same box size and box content (Figure S1a). The box needs to be large enough to avoid contact of the adsorbate with the surface during the solution run. However, large boxes result in high values and large fluctuations of the total energy which require extra simulation time to compute the relatively small energy difference $\Delta \boldsymbol{E} = \boldsymbol{E}_1 - \boldsymbol{E}_2$ between simulation 1 and simulation 2 with statistically acceptable errors (Figure S1a). The time dependence on the number of particles $\boldsymbol{N}$ is typically on the order $\boldsymbol{N}^2$ for summations of Coulomb interactions using the Ewald method and for summations of van-der-Waals interactions using spherical cutoffs, and on the order $\boldsymbol{N}\cdot\ln\boldsymbol{N}$ for summation of Coulomb interactions using the PPPM method.

Method 1 is less efficient due to the inclusion of many water molecules in the surface run, and due to the inclusion of the surface atoms and surrounding water molecules in the

solution run (Figure S1b). This introduces particular computational overhead when the adsorption of a series of molecules on the same surface is of interest. In the presence of usual periodic boundary conditions, these issues of method 1 can be circumvented by taking the additivity of intermolecular interactions into account. As shown earlier,[41] the interaction of polar but overall charge neutral molecules or crystals becomes almost negligible at distances greater than 3 nm so that larger simulation boxes in Figure S1a can be split into multiple boxes of ~5 nm height as shown in Figure S1b. This partition of the computation boxes leads to method 2.

**S2.2. Method 2 − Efficient Approach.** In the second scheme (Figure S1c), a total of four calculations with smaller boxes are required which is approximately twice as fast as two calculations with larger boxes using Ewald procedures or spherical cutoffs for Lennard-Jones interactions ($\boldsymbol{t}(\boldsymbol{N}) \sim \boldsymbol{N}^2$). For computational screening of additional adsorbates on the same surface, only two additional calculations per adsorbate are required to obtain $\boldsymbol{E_{Surf+A+H2O}}$ and $\boldsymbol{E_{A+H2O}}$ while the values for $\boldsymbol{E_{H2O}}$ and $\boldsymbol{E_{A+H2O}}$ remain the same. Assuming a dependence of simulation time $\boldsymbol{t(N)}$ on the number of atoms $\boldsymbol{N}$, a box size of $\boldsymbol{2N}$ in Fig. S1a, and about half the box size $\boldsymbol{N}$ in Fig. S1c, the computation of adsorption energies for $\boldsymbol{k}$ peptides on the same surface takes the relative time $\frac{2\boldsymbol{k}+2}{2\boldsymbol{k}} \cdot \frac{\boldsymbol{t}(\boldsymbol{N})}{\boldsymbol{t}(2\boldsymbol{N})}$. For example, method 2 will screen 20 peptides in 26% of the time compared to method 1 in a simulation with $\boldsymbol{t}(\boldsymbol{N}) \sim \boldsymbol{N}^2$ (Ewald or spherical cutoffs), and in less than 50% of the time compared to method 1 in a simulation with $\boldsymbol{t}(\boldsymbol{N}) \sim \boldsymbol{N} \ln \boldsymbol{N}$ (PPPM summations).

A further advantage of method 2 over method 1 is the reduction of the total energy and its standard deviation, which lowers the standard deviation of computed adsorption energies on an absolute scale. Possible interferences from the surface in the solution run in method 1 are also

eliminated, and method 2 equally provides access to thermodynamic quantities including energies, entropies, and free energies of adsorption. The computation of entropy $\Delta \boldsymbol{S}$ (using $\boldsymbol{A} = \boldsymbol{U} - \boldsymbol{TS}$ or other method) and free energy $\Delta \boldsymbol{A}$ is more time-consuming than that of the energies, however, because very well resolved histograms of the energy distribution are needed or multiple simulations for each system to facilitate thermodynamic integration, respectively.

The application of either method, provided the box size is large enough to eliminate finite size effects and simulations are allowed to reach equilibrium, leads to identical results. Simulations are best performed using the NVT ensemble and additive molecular volumina, i.e., predefined densities for each constituent such as metal atoms, water molecules, and peptides. Then, for example, using the same cross section ($\boldsymbol{A} = \boldsymbol{xy}$) of the box, the box height ($\boldsymbol{z}$) is incrementally additive for every component added. To compute differences in thermodynamic quantities, the simulation temperature must be constant or corrected to the same value using the heat capacity of each box (as derived in the simulation).

(a) **Method 1**

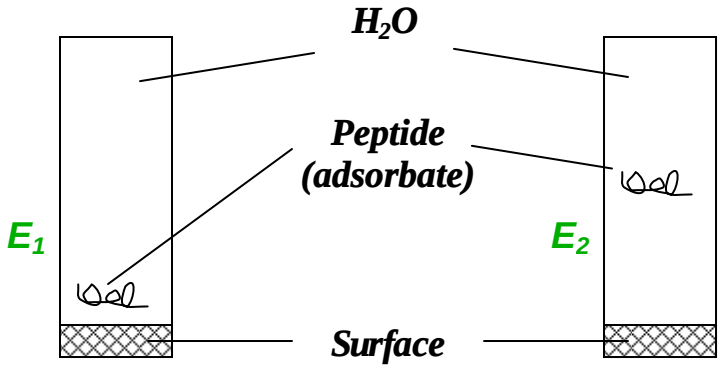


Surface Solution

$\Delta E = E_1 - E_2$

(b) Decomposition as

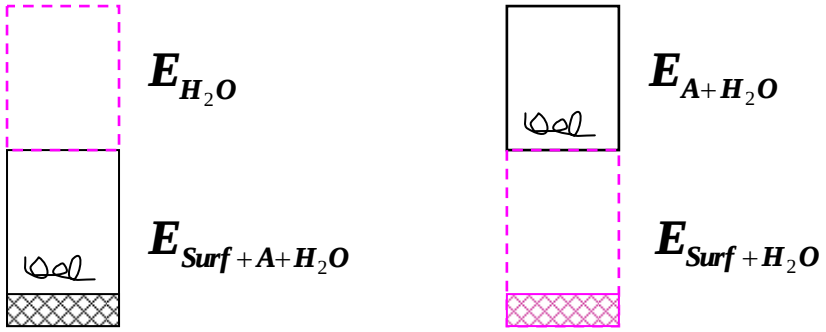


(c) **Method 2**

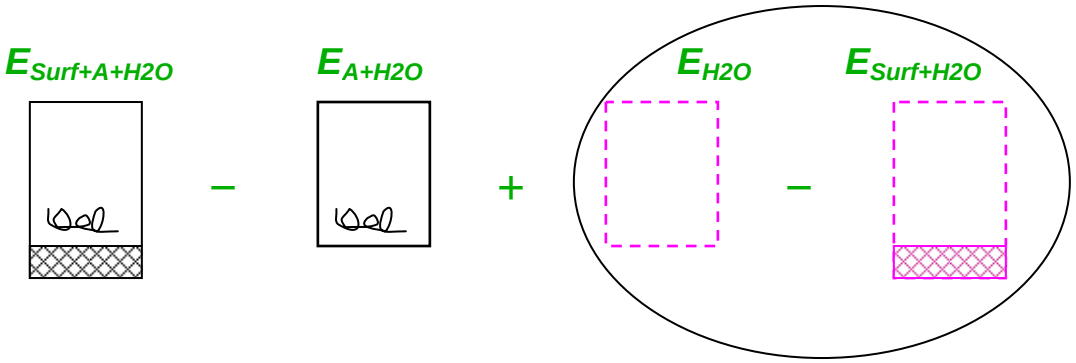


Constant term = $- E_{SL} -$

**using**

$E_{SL} =$

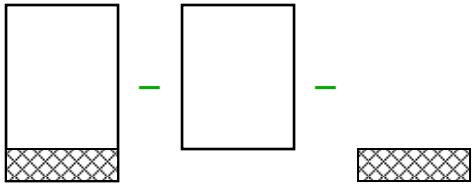

$\Delta E = E_{Surf+A+H2O} - E_{A+H2O} + E_{H2O} - E_{Surf+H2O}$

$\Delta S, \Delta G$ analogous

**Fig. S1.** Computation of adsorption energies under periodic boundary conditions (illustrations in 2D for simplicity). (a) Method 1 involves the calculation of average energies in two simulation boxes with the adsorbate on the surface and in solution. (b) Decomposition into smaller boxes for reduced computation time and lower fluctuation in computed energy differences. (c) Method 2 involves four smaller boxes and is more efficient than method 1, particularly for screening many molecules on the same surface.

## S3. Computational Details

**S3.1. Models of the Peptides, Water, and the Metallic Substrates.** Atomistic Models of the peptides were build from scratch using the amino acid sequences and protonation state at pH = 7 outlined in Table 1. In addition to the possible presence of counterions (Flg-$Na_3$, Flgd-$Na_2$, Pd2-Cl, Pd4-Cl), all peptides are used in their zwitterionic form. Models of the peptides in different backbone conformations ($\alpha$-helix, extended, random coil) were prepared with the help of the Hyperchem visualizer,[47] as well as by manual drawings (random coil) using the Materials Studio builder[48] and simple energy minimization. For water, we employ the standard SPC model implemented in the consistent valence force field (CVFF).[49]

Models of the fcc metals were constructed from the unit cell parameter $\boldsymbol{a}_0$ and the atom positions (0,0,0), (1/2,1/2,0), (1/2, 0, 1/2), (0, 1/2, 1/2).[35] The fcc unit cell and related supercells yield {100} surfaces along the Cartesian coordinate axes. To construct {111} surfaces, an equivalent larger cell was build as $\frac{\sqrt{2}}{2}\boldsymbol{a}_0 \times \frac{\sqrt{3}\sqrt{2}}{2}\boldsymbol{a}_0 \times \sqrt{3}\boldsymbol{a}_0$ with the atom positions (0, 0, 0), (1/2, 1/2, 0), (0, 1/3, 1/3), (1/2, 5/6, 1/3), (1/2, 1/6, 2/3), (0, 2/3, 2/3). {111} surfaces are then obtained perpendicular to the z axis.[29] The Pd-Au {111} bimetal interface was constructed starting with the Au supercell and replacement of half the atoms by Pd. The lattice constants are very similar (4.0782 Å vs 3.8903 Å) so that the scale of the simulation box (3 nm) does not lead to dislocations; a fractional offset of the Pd lattice positions from the nominal Au lattice positions was observed in the course of the simulation.

Complete start structures consist of the inorganic substrate, the peptide, and water, or subsets thereof with three-dimensional periodic boundary conditions (see Figure S1c). The structures for each set of simulations were assembled from slabs of the metal substrate, pre-equilibrated assemblies of 1000 water molecules (2000 water molecules using method 1 in

Figure S1a), and one peptide chain using the Materials Studio graphical interface.[48] The initial conformations of the peptide chains were obtained from the build of various conformations, the result of the solution run, as well as from pre-equilibrated peptide conformation on the metal surface in vacuum (without solvent). The setup of the hybrid structures assumes a density of 1000 kg/m$^3$ for all liquid phases such as water and peptide solutions, and the exact density of the metal consistent with unit cell parameters. The box dimensions are typically 3 nm × 3 nm × ***z*** whereby the box height ***z*** amounts to ≥1.2 nm for metal substrates, ≥3.5 nm for water, and ≥3.5 nm for the aqueous solutions of the peptides. The size was chosen such that 25% to 40% of the surface area is covered by the peptide, close to experimental conditions. This comparatively low surface coverage for a single peptide chain in the simulation box also reduces finite size effects to a tolerable level. The peptides can be initially superimposed onto the water slab; subsequent energy minimization removes close contacts with only modest distortions of the initial secondary structure. The concept of additive molecular volumes and the choice of a benchmark density for every component is required for NVT simulations according to Figure S1; computed adsorption properties are not affected if benchmark densities are changed consistently in all simulations in a range of ±1%.

**S3.2. Force Field Parameters for Peptides and Metals.** At the classical atomistic level, several force fields with good parameters for peptides and water are available, e.g., AMBER, CHARMM, CVFF, OPLS-AA, PCFF, and compatible parameters for inorganic structures have been recently developed.[29,37−41] The improvement of Lennard-Jones parameters for fcc metals leads to better than 10% agreement of surface and interface properties with experiment for fcc metals[29,32−36] which is essential to understand sensitive interfacial adsorption processes. In contrast, earlier metal parameters in force fields were associated with deviations in excess of

100% and result in wide gaps between computed adsorption properties and actual interfacial interactions in experiment.[3,23–27] In this paper, we employ the consistent valence force field (CVFF)[48,49] extended for accurate Lennard-Jones parameters for fcc metals (Ag, Al, Au, Cu, Ni, Pb, Pd, Pt).[29]

This extended version of CVFF, therefore, contains the existing parameters for the peptides and water[48,49] as well as new, accurate parameters for fcc metals.[29] The potential energy expression with no cross-terms and no morse potential is employed:

$$\boldsymbol{E}_{pot} = \boldsymbol{E}_{bond} + \boldsymbol{E}_{angle} + \boldsymbol{E}_{torsion} + \boldsymbol{E}_{out-of-plane} + \boldsymbol{E}_{Coulomb} + \boldsymbol{E}_{vdW} \quad \text{(S1)}$$

$$= \sum_{ij \text{ bonded}} \boldsymbol{K}_{r,ij}(\boldsymbol{r}_{ij} - \boldsymbol{r}_{0,ij})^2 + \sum_{ijk \text{ bonded}} \boldsymbol{K}_{\theta,ijk}(\theta_{ijk} - \theta_{0,ijk})^2 + \sum_{ijkl \text{ bonded}} \boldsymbol{V}_{\phi,ijkl}[1 + \cos(\boldsymbol{n}\phi_{ijkl} - \phi_{0,ijkl})]$$

$$+ \boldsymbol{E}_{oop} + \frac{1}{4\pi\varepsilon_0\varepsilon_r} \sum_{\substack{ij \text{ nonbonded} \\ (1,2 \text{ and } 1,3 \text{ excl})}} \frac{\boldsymbol{q}_i\boldsymbol{q}_j}{\boldsymbol{r}_{ij}} + \sum_{\substack{ij \text{ nonbonded} \\ (1,2 \text{ and } 1,3 \text{ excl})}} \varepsilon_{ij}\left(\left(\frac{\boldsymbol{r}_{0,ij}}{\boldsymbol{r}_{ij}}\right)^{12} - 2\left(\frac{\boldsymbol{r}_{0,ij}}{\boldsymbol{r}_{ij}}\right)^{6}\right)$$

Equation (S1) shows the additive energy terms for quadratic bond stretching $\boldsymbol{E}_{bond}$, quadratic angle bending $\boldsymbol{E}_{angle}$, a one-term torsion potential $\boldsymbol{E}_{torsion}$, quadratic out-of-plane deformation $\boldsymbol{E}_{out-of-plane}$, electrostatic energy $\boldsymbol{E}_{Coulomb}$, and a 12-6 Lennard-Jones potential $\boldsymbol{E}_{vdW}$ for van-der-Waals interactions. Nonbond interactions between 1,4 covalently bonded atoms are included to 100% and geometric combination rules apply for Lennard-Jones parameters between different atom types. A critical advantage over earlier models is the accurate 12–6 Lennard-Jones potential for fcc metals. Computed cell parameters for the metals approach experimental values within 0.2% deviation, computed surface tensions for the {111} surfaces of the metal fall within 1-5% of the experimental values at 298 K (equal to the uncertainty in experiment), and the computed surface energy anisotropy between the {111} and {100} metal surfaces compares favorably with experimental data.[29,33,34] Computed metal-water interfacial tensions are on average 10% to 15%

lower than expected from experimental data according to the Young equation.[29] A lower interface tension might have some justification, however, due to attractive polarization effects as the Young equation only provides an upper bound. In detail, polarization will be discussed in a separate contribution. In summary, computed surface energies using metal parameters in earlier semiempirical force fields were associated with errors on the order of 100% so that the present semi-quantitative treatment represents an improvement of between one and two orders of magnitude in accuracy. Remaining sources of uncertainties are (1) polarization effects, (2) the approximate nature of the energy model, specifically limitations of the SPC water model and of the peptide parameters, (3) geometric combination rules of the 12-6 Lennard-Jones parameters, (4) and the inability of the force field to consider covalent contributions, such as major shifts in electron density, to adsorption.

**S3.3. Simulation Protocol.** The programs Discover[48] and LAMMPS[50] were used to carry out molecular dynamics (MD) simulations. Typically, we started with a short energy minimization for 200 steps using the conjugate gradient method, and then carried out NVT molecular dynamics. A time step of 1 fs, the Verlet integrator, the Anderson or the Nose thermostat at 298.15 K, a van-der-Waals cutoff at 1.2 nm, Ewald summation of Coulomb interactions with high accuracy ($10^{-6}$ kcal/mol), or PPPM summation of Coulomb interactions with high accuracy ($10^{-6}$ kcal/mol) were employed. The analysis of adsorption energies and chain conformations followed as a post-processing operation after typical simulation times of 5 ns to 10 ns, corresponding to 5 to 10 million time steps. For the analysis, the first 1 ns or more of the trajectory was discarded to take into account only the parts of the trajectory with steady energies and thermodynamically significant conformations. We note thermodynamic averages,

as well as the visual and statistical inspection of complete trajectories are required to understand conformational changes so that representative snapshots are intended for guidance only.

A bottleneck is the generation of a Boltzmann average of equilibrium conformations of the peptides on the surface. While the modest length of the peptides up to 12 amino acids does not excessively complicate this goal, several start conformations that are distinct from each other, such as helix, outstretched, random coil, and optimized structures in vacuum were required. Solution structures converge to consistent results, however, on the metal surfaces with particularly strong adhesion, we cannot be certain that the global minimum energy has been reached in every case as relaxation times exceed 10 ns. However, the deviation in adsorption energies is mostly in a range of ±5 kcal/mol for different start structures in independent simulations which is less than 10% of the strongest adsorption energies seen. Besides, reference to coarse-grain models and Monte Carlo algorithms to pre-equilibrate the structures in a sequential, reversible two-scale approach may not result in major improvements in sampling as the competition of water and peptide on the surface and specific polar chemistries of side groups are difficult to capture in simplified models.

An important aspect in the computation of adsorption energies was the adjustment of the average total energy for each simulation to the same reference temperature (298.15 K) using the heat capacity of the simulation box. Even small temperature differences (<0.1 K) between individual calculations (Figure S1) cause noticeable energy differences (<2 kcal/mol) and could introduce errors in computed adsorption energies.

## S4. Additional Evidence on the Binding Mechanism from Previous Simulations

Additional evidence for the proposed binding mechanism by earlier computational results at various length scales is described in the following.

**S4.1. Ab-initio methods.** Ab-initio methods have been employed to study peptide fragments such as amino acids or water in contact with fcc metals at the smallest level without significant dynamics or solvation.[21,22,24,26,28] In a benchmark study, Haftel et al.[21] compared the reliability of tight-binding (TB), electron density functional methods (DFT), embedded atom models (EAM), and modified embedded atom models (MEAM) to compute surface tensions of several fcc metals (Rh, Ir, Ni, Pd, Pt, Au). The methods exhibit scatter by a factor of two among each other, and typical deviations from experiment are ~20% in each method with individual deviations up to 50% both above and below experimental values. The reliability is therefore a problem and must be taken into account in the discussion of DFT results, as well as difficulties to combine DFT methods with classical force fields to simulate the dynamics of peptides with explicit solvent molecules in solution.

Water adsorption and layering on transition metal surfaces was studied by Vassilev et al.[22] using Born-Oppenheimer DFT. On Rh {111} and Pt {111} surfaces, a planar orientation of water molecules is found, and the adsorption energy of single water molecules in vacuum at low surface coverage was computed as 8.6 and 6.9 kcal/mol, at a higher coverage with a water bilayer, 13.1 kcal/mol and 13.1 kcal/mol for Rh and Pt surfaces. Schravendijk et al.[24] also found a planar coordination of water molecules on the metal surfaces and computed slightly higher adsorption energies of single water molecules of 9.7 and 8.1 kcal/mol on Rh {111} and Pt {111} surfaces, as well as 2.3 and 7.6 kcal/mol on Au {111} and Pd {111} surfaces. Classical MD simulation (section S3) agrees with the preference for a planar orientation and adsorption

energies of 4.4 and 5.4 kcal/mol are computed on the Au {111} and on the Pd {111} surface at <5% surface coverage (calculation as in Figure S1a with one water molecule as adsorbate in vacuum).[29] These values agree with lower surface tensions of Au and Pd versus Rh and Pt;[32] the gap in DFT calculations between the Au {111} and Pd {111} surface yet remains to be explained on physical grounds.[24] Experimental measurements of contact angles indicate 0º and, therefore, hydrophilic properties of both clean Au and Pd surfaces,[36] in agreement with attraction of water to the metal surfaces in the computation. Further, dual-scale simulations of benzene adsorption on Ni {111} and Au {111} surfaces including a few explicit water molecules were carried out by DFT and Car-Parrinello ab-initio MD molecular dynamics as well as specialized Lennard-Jones and Morse potentials for a classical description of the interaction with the metal. Taking into account competition between a few water molecules and the benzene solute, the adsorption energy of benzene in solution on the Ni {111} surface was computed as 9.6 kcal/mol, slightly stronger adsorption was found on the Pd {111} surface, and a preference for desorption was predicted on the Au {111} surface. However, the surface tension of the metals was not validated in these models and the few included water molecules are a crude approximation of a solvation shell. Nevertheless, the binding energy agrees with the order of magnitude for aromatic amino acids (Table 2 and Table 4), and a weaker attraction of benzene (in Phe) to the Au {111} surface is also observed in our study. Our results indicate still adsorption in agreement with experimental data (section 5.1).[4,7,8] It may be alternatively possible that phenyl rings are positioned flat on the surface only in order to provide sufficient “contact area” for neighboring parts of the molecule which are factually involved in an adsorption process. Schravendijk’s method[24] was further extended into a highly specialized force field description for the interaction of selected hydrated amino acids with a Ni {111} surface.[26] A new extensive set of parameters would be required for

every additional amino acid and every additional metal. Meanwhile, the validation of the metal surface energy and the physical justification of the numerous parameters remain unclear, and incompatibility with existing biomolecular force renders the approach less practical. Therefore, atomistic simulation with extended force field engines as presented in this paper yields results of the same, if not better, quality, and is simpler, faster, and more widely applicable.

Ghiringhelli et al.[28] studied Phe adsorption in vacuum on {111} surfaces of fcc metals using DFT. Strong adsorption of −30 to −25 kcal/mol (Pt, Ni, Pd) and weaker adsorption of −12 to −7 kcal/mol (Cu, Ag, Au) was found. For Cu, Ag, Au, the phenyl ring is not in close contact with the surface. Although water was absent in this study, the range of values is similar to those inferred from the force-field based simulation (Tables 2 and Table 4);[30] a lesser attraction of the phenyl ring to the Au {111} surface compared to the Pd {111} surface is observed in our method as well. Hong et al.[31] have shown by further DFT calculations in vacuum that charge transfer is possible on Au and Pd surfaces. Up to −0.65e could be transferred per negatively charged residue such as $CO_2^-$ of Asp over numerous electron accepting superficial Au atoms in vacuum (Table 3). In aqueous solution, however, the presence of water molecules as a solvent of similar polarity diminishes the amount of charge transfer from a single $CO_2^-$ group which would be more challenging to analyze using this method. Among Asp, Lys, Arg, Ser, Pro, and Val, the strongest binding residue in vacuum has been Asp by a considerable margin (−57 kcal/mol), followed by Lys (−27 kcal/mol) and Arg (−19 kcal/mol), and almost no binding was found for Pro and Ser. While the values will be substantially smaller in aqueous solution, this ranking coincides with the force-field based simulation (Tables 2 and 4).

**S4.2. Force-field based simulations.** Sarikaya et al.[3,S1] carried out classical molecular dynamics simulations of large proteins (>40 amino acids) on Au {111} and {112} surfaces with

a number of heavy approximations which weigh on the reliability of the results: (1) The proteins were placed in a dielectric continuum so that explicit water molecules and hydrogen bonds are absent. (2) The surface properties of Au according to the chosen Lennard-Jones parameters were not validated which adds uncertainty in excess of 100% to adsorption energies and affects the molecular mechanism of adsorption of the peptide.[29] (3) The thickness of the surfaces was restricted to only 3 atomic layers (6 Å) which is shorter than the range of interactions between the metal atoms (at least 10−12 Å). Comparisons relative to experiment are rather difficult under these conditions, and further simulations of peptides on metal surfaces using this approach lead to a number of questionable specific results.[23] An interesting outcome, however, is the response of peptides to gross surface features such as ridges in {110} surfaces. A subsequent study by Kantarci et al.[25] extended the approach using an all atom representation of peptides and water on Pt {111} surfaces. This represents a more realistic model, however, the Lennard-Jones parameters for the metal according to the unmodified CVFF overestimate the Pt surface tension by 101% relative to experiment and modify the interfacial structures and adsorption processes;[29] the thin metal layer also introduced residual interactions between water molecules above and below the metal slab. Under these severe approximations, Ser, Thr, Arg, and Pro were found in proximity to the metal surface (Pt). Overall, earlier all atom models may not have been reliable enough for quantitative or firm qualitative conclusions.

## References

S1 Braun, R.; Sarikaya, M.; Schulten, K. S. ***J. Biomater. Sci.*** **2002**, ***13***, 747–758.